On the Adsorption Process in Polymer Brushes: A Monte Carlo Study

A. Kopf,* J. Baschnagel, J. Wittmer,† and K. Binder

Institut für Physik, Johannes-Gutenberg Universität, 55099 Mainz, Germany

Received July 24, 1995; Revised Manuscript Received October 30, 1995[⊗]

ABSTRACT: The adsorption process of the single polymer chain in a polymer brush of varying surface coverages is studied by means of Monte Carlo simulations of the bond-fluctuation lattice model. Only the end monomers can adsorb at the grafting surface, whereas inner monomers interact repulsively with it. The brush builds up a steric hindrance which forces the penetrating polymer to stretch strongly and which is responsible for small adsorption probabilities at surface coverages close to the overlap density. The final step of the adsorption process is determined by a fluctuation of the end monomer around its average position, which is comparable to the initial step of the desorption process.

I. Introduction

Polymer brushes[1] are thin polymeric films consisting of (linear) chains, one end of which is attached to a surface. Since these polymer brushes find many technical applications (stabilization of colloids,[2] adhesion and lubrication[3,4]), they have attracted a lot of research interest in the last years.[1,5] A rather detailed picture of their equilibrium properties has thus emerged. Depending on the value of the grafting density σ_g, one distinguishes between the *mushroom* and the *semidilute* regimes. In the mushroom regime the grafted chains do not overlap and essentially behave as isolated chains in solution. The relevant length and time scales are thus the radius of gyration $R_g \propto N^{\nu}$ and the Rouse relaxation time $\tau_r^* \propto N^{1+2\nu}$ (if hydrodynamic interactions are unimportant as in the present simulation), where N is the chain length and $\nu \approx {}^3/_5$ for good solvent conditions. When the grafting density crosses the threshold $\sigma_g^* \approx 1/R_g^2$, the chains start to overlap and the resulting excluded volume interaction forces them to stretch perpendicular to the surface. In this semidilute regime the height h of the brush is the largest length in the system, followed by the chain extension parallel to the surface. To these length scales correspond the relaxation time of the chain ends τ_r and the internal relaxation time of the chain conformation τ_d, which depend on σ_g and increase with chain length as $\tau_r \propto N^3$ and $\tau_d \propto N^2$. These results were predicted by theory[8−13] and could be confirmed by experiments[6,7,14] and computer simulations.[5,15−20] The general view is that a semidilute polymer brush can be described by a *blob picture*[8,9] in which the excluded volume interaction becomes negligible outside of a certain region, called a "blob", around a chain. Whereas at the surface the blob size $\xi(0)$ is determined by the grafting density (i.e., $\xi(0) = [1/\sigma_g]^{1/2}$), it increases toward the edge of the brush so that the portion of the polymer in the last blob behaves as in dilute solution.[19,28,34] The size d_{fl} of this last blob can be neglected in the theoretical scaling limit ($N \to \infty$, $\sigma_g \to 0$, but $\sigma_g N^{2\nu} \gg 1$), but may become noticeable in either experiments[6,7,14] or simulations.[5,28]

Contrary to the just described equilibrium properties of polymer brushes, the nonequilibrium properties of brush formation and degradation are not as well established. The formation of a brush from a solution of end-functionalized polymers was investigated by experiments[21,22] and simulations.[26,27] These studies showed that the formation of a brush is a two-stage process. The initial stage is a (fast) diffusion-limited process in which the grafting density increases as $\sigma_g \propto t^{1/2}$, whereas at later times the already anchored chains sterically hinder the further adsorption process, leading to an exponential time behavior. This behavior is also predicted theoretically.[24,25] Another characteristic feature of the adsorption process is that short chains quickly replace already grafted long chains of the same type, which was found in experimental,[23] theoretical,[25] and simulational studies.[26,27] This results directly from the weaker barrier seen by short chains approaching the brush whereas long chains even with a higher adsorption energy first have to overcome the higher steric hindrance of the existing polymer film. Therefore for the competitive adsorption process, a disparity in chain length seems to be much more important than one in the grafting energy.[25−27] For practical interests, the grafting energy is roughly $E_g \approx 10 k_B T$ so chain replacement is unlikely but possible.

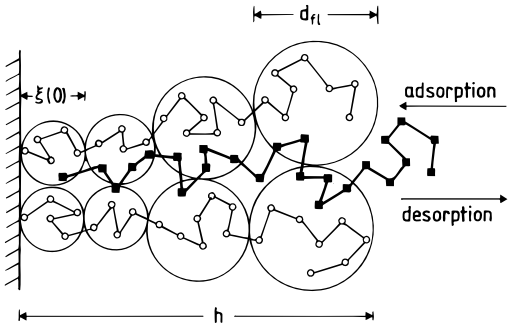

Figure 1. Schematic illustration of the adsorption (desorption) process as studied in the present work. A single chain enters (leaves) a polymer brush. If its end monomer touches (is cut off) the wall, the chain adsorbs (desorbs) irreversibly. In addition, the brush height h, the size of first blob $\xi(0)$, and the size of the last blob d_{fl} are drawn in.

Whereas the cited studies concentrated on more macroscopic quantities such as σ_g, the microscopic mechanism of the desorption process (see Figure 1) was investigated by dynamic Monte Carlo simulation in ref 28. This investigation analyzed the dynamics of the desorption in two ways. On the one hand, a randomly chosen chain was cut off the wall and its diffusion out

* To whom correspondence should be addressed.
† Present address: Department of Physics and Astronomy, University of Edinburgh, King's Building, Mayfield Road, Edinburgh EH9 3JZ, UK.
⊗ Abstract published in *Advance ACS Abstracts,* January 15, 1996.

0024-9297/96/2229-1433$12.00/0

of the brush was monitored. On the other hand, a finite grafting energy E_g was introduced for all chains so that desorption of a chain occurs with probability $\exp[-E_g/k_BT]$. Both approaches yield the following picture of the desorption process: The desorption of an initially grafted monomer is a *local* process which is independent of N. As long as the monomer is in the first blob close to the surface, the probability for readsorption is large. The desorption time depends on E_g and on the time that the end monomer needs to diffuse through the first blob. The end monomer has to diffuse through several blobs before the chain's center of mass moves significantly. When the center of mass starts to move, it is expelled out of the brush with a *constant* velocity until it reaches the position $h - d_{fl}$. Then it diffuses freely and the conformation of the chain is isotropic.

Since such a detailed picture of the desorption process is available and since the adsorption process is the corresponding reverse process, the aim of the present paper is to study the microscopic properties of the adsorption of a single chain in a brush and to relate the results to those of the desorption. The outline of the paper is as follows: In section II the model and the details of the simulation are described. Section III presents the results of the simulation. The last section gives a brief summary of the main results.

II. Simulation Method

The Monte Carlo simulation was performed with a coarse-grained lattice model, the bond-fluctuation model, which is described elsewhere.[33] This model has been used in many previous studies of the static and dynamic properties of polymer brushes under various solvent conditions[15,16,20,26,34] and of the chain desorption process from a brush.[28,34,35] Since desorption and adsorption are inversely related to each other, we want to work with exactly the same model in order to compare our data with the results from ref 28 whenever possible.

For the analysis of the adsorption process, we first monitored the motion of a single chain when it approaches the wall to which a polymer brush (with chains of the same length) of varying grafting densities σ_g is anchored. Adsorption takes place if an end monomer jumps from the lattice layer $z = 1$ to the wall at $z = 0$. For the other monomers inside of the chain, the wall represents a purely repulsive potential. In addition to the wall at $z = 0$, a cut-off border $z^b_{cm} \gg 0$ is introduced to make the simulation more efficient. As soon as the polymer reaches the border with its center of mass, it is removed from the lattice and a new simulation is started with an equilibrated polymer at $0 \ll z^a_{cm} < z^b_{cm}$ (the relaxation time of the conformation of a single chain is given by $\tau_r^* \approx 5N^{1+2\nu}$ [28]).

The properties of a polymer brush are determined by the length N and by the number M of grafted polymers on the surface, the size of which was (mostly) chosen to be $L_x \times L_y = 30 \times 30$ (in units of the lattice constant). We worked with $N = 10$, 20 (for both the adsorbing polymer and the brush) and with $M = 10$, 20, 30, 40 ($N = 10$) and $M = 0$, 1, 6, 10, 12, 14, 16, 20 ($N = 20$) chains on the surface. This corresponds to a surface coverage of $\sigma = 0.044$, 0.088, 0.133, 0.177 ($N = 10$) and $\sigma = 0$, 0.0044, 0.026, 0.044, 0.053, 0.062, 0.071 ($N = 20$). For the introductory study of the adsorption of a single chain on an empty surface (i.e., $\sigma = 0$), the simulation box had the linear dimensions $L_x \times L_y \times L_z = 100 \times 100 \times 100$, whereas $L_x \times L_y \times L_z = 30 \times 30 \times 100$ was used for finite surface coverages (all lengths are measured in units of a lattice constant). The relation between the surface coverage and the grafting density is given by

$$\sigma = 4\sigma_g = 4M/L_xL_y \tag{1}$$

since a monomer of the bond-fluctuation model corresponds to a unit cell of the simple cubic lattice and thus occupies four lattice sites on the grafting surface. When σ is small, chains grafted at different places of the surface do not overlap and exhibit a mushroom-like shape (mushroom regime). The grafted polymers start to overlap when $\sigma^* R_g^2 = 0.14$ for the bond-fluctuation model,[28] where R_g is the radius of gyration of an isolated chain. $\sigma^* R_g^2$ marks the beginning of the crossover from the mushroom to the semidilute regime, which is reached when $\sigma R_g^2 \approx 0.53$ for the bond-fluctuation model.[28] Using $R_g \approx 1.05N^{\nu}$ [28,36] (i.e., $R_g(N=10) \approx 4.2$, $R_g(N=20) \approx 6.3$), the crossover occurs for $0.032 \le \sigma \le 0.121$ for $N = 10$ and $0.014 \le \sigma \le 0.053$ for $N = 20$, respectively. Therefore our simulations cover the range from the mushroom to the onset of the semidilute regime.

III. Analysis of the Adsorption Process

As mentioned in the previous section, the adsorption process was first studied by monitoring the approach of a single chain to the wall. Of particular interest are the average adsorption time, the position of the center of mass and of the other nonadsorbed end monomer, and the chain conformation at the moment of adsorption. To investigate the chain conformation, the components of the radius of gyration were measured

$$R^2_{g,x} = \frac{1}{N}\sum_{j=1}^{N}(x_j - x_{cm})^2, \qquad R^2_{g,y} = \frac{1}{N}\sum_{j=1}^{N}(y_j - y_{cm})^2,$$
$$R^2_{g,z} = \frac{1}{N}\sum_{j=1}^{N}(z_j - z_{cm})^2 \tag{2}$$

Here x_j, y_j, and z_j are the components of the position vector of the jth monomer and x_{cm}, y_{cm}, and z_{cm} are the components of the position vector of the polymer's center of mass.

In order to obtain a detailed picture of the adsorption process, it is, however, important not only to determine the configurational properties of the polymer at the moment of adsorption but to record the time evolution of these properties during the whole process. When investigating the motion of the polymer toward the wall and inside the brush, one faces the problem that the moment of adsorption is undetermined. Due to the stochastic motion of the polymer, it is impossible to predict precisely when adsorption will occur (if it does at all during the available simulation time). A possible way to deal with this difficulty is to examine the adsorption process in reverse. This means that the moment of adsorption is defined to be the time origin $t = 0$ so that the motion of the polymer and the change of its conformation are studied as a function of negative times; e.g., −500 MCS means 500 MCS before adsorption (MCS is an abbreviation for "Monte Carlo steps", the intrinsic time unit of the simulation; a MCS is defined as the time needed to give every monomer in the system the chance to move once on average). This is a sensible definition, since the time origins of adsorption and desorption are then comparable. Please note, however, that they do not coincide exactly. This is due to the fact that the configurational properties of the

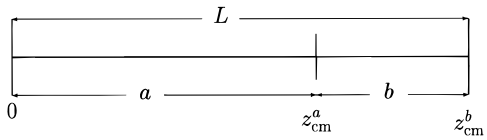

Figure 2. One-dimensional random walk with absorbing boundaries at 0 and z^b_{cm}. The walker starts at z^a_{cm}.

adsorbing chain were not recorded at every MCS, but in regular intervals of 100 MCS's only. Therefore the instant of adsorption is determined with an uncertainty of 100 MCS's, which passes on to the other times before the adsorption. Of course, it would be possible to eliminate this uncertainty by monitoring every MCS. This was not attempted here due to computational reasons.

A. Adsorption on an Empty Surface. The center of mass of a free polymer of chain length $N = 20$ is placed at the starting point $z^a_{cm} = 15$, 20, 25 above the wall, whereas the cut-off border $z^b_{cm} = z^a_{cm} + b$ was chosen with $b = 5$, 10, 15, 20, 30 lattice constants (see Figure 2). The variation of z^a_{cm} and z^b_{cm} was done to obtain a feeling for a suitable choice of these parameters in the subsequent analysis of the adsorption process in polymer brushes and to check the correctness of the programs by comparing the simulation results with an analytical random walk calculation. As long as the polymer is not very close to the wall (i.e., as long as the z-position of the center of mass is larger than R_g), its dynamic behavior is adequately described by the random-walk-like motion of the center of mass. Therefore it should be possible to calculate the average adsorption time, at least approximately, from a one-dimensional random walk of a point particle with two absorbing boundaries (see Figure 2). In the context of random walks, the average adsorption time is called "first-passage time". The first-passage time to reach the left boundary $\langle t_{left} \rangle$ is defined by[37]

$$\langle t_{left} \rangle = \frac{1}{\pi_{left}} \int_0^\infty t f_{left}(t)\, dt \qquad (3)$$

where $\pi_{left} = b/L$ (see Figure 2) is the splitting probability for absorption at the left boundary and $f_{left}(t)$ is the corresponding absorption probability at time t. For a one-dimensional random walk, $f_{left}(t)$ is given by Fürths' formula[38,39]

$$f_{left} = \frac{2\pi D}{L^2} \sum_{n=1}^{\infty} n \exp\left[-\frac{n^2\pi^2 D t}{L^2}\right] \sin\frac{n\pi a}{L} \qquad (4)$$

where D is the diffusion coefficient of the particle. Using this expression in eq 3,one obtains

$$\langle t_{left} \rangle = \frac{1}{6D(L-a)}[a^3 - 3a^2 L + 2aL^2] \qquad (5)$$

By exchanging a with b, eq 5 yields the first-passage time $\langle t_{right} \rangle$ for the absorption at the right boundary.

When trying to apply eq 5 to our simulation data, the problem arises that the absorbing boundaries are not treated symmetrically in the simulation, contrary to the analytical random walk problem. Whereas the cut-off border responds to the motion of the center of mass and is thus comparable to the boundary condition of the random walk problem (i.e., $z^b_{cm} - z^a_{cm} = b$), the adsorbing wall is sensitive to the touch of an end monomer. To account for this different condition at the wall, one can

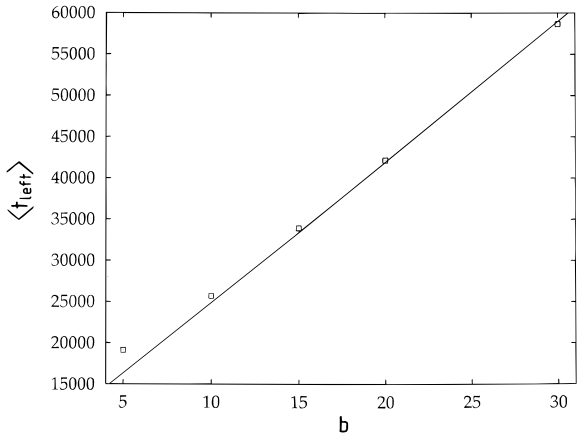

Figure 3. Comparison of the simulation results for the mean adsorption time of a single chain ($N = 20$) on an empty surface with the random walk formula (eq 5) for the first-passage time. b is the difference between the cut-off border z^b_{cm} and the starting point of the polymer z^a_{cm} ($z^a_{cm} = 20$ lattice constants above the wall for the present case; see Figure 2 for further explanation). Visible are deviations from the fit for small values of b, since the point-particle approximation becomes invalid when $b \approx R_g \approx 6.3$.

define a shift constant k as

$$a = z^a_{cm} - k \qquad (6)$$

which introduces an imaginary absorbing boundary for the center of mass k lattice spacings above the wall. Intuitively, one can expect k to be equal to the average z-position of the center of mass at the moment of adsorption. In order to check this expectation, we calculated k from the splitting probability $\pi_{left} = b/L = b/(b + z^a_{cm} - k)$. Indeed, the resulting value $k \approx 11$ coincides with the average z-position of the center of mass at the moment of adsorption within the error bars. Having determined k, we can use this result to estimate the diffusion coefficient of the polymer by[39]

$$D = \frac{(z^a_{cm} - k)b}{2(\pi_{left}\langle t_{left} \rangle + \pi_{right}\langle t_{right} \rangle)} \qquad (7)$$

which yields $D = 0.0017$. This agrees very well with the value of the diffusion coefficient obtained in a simulation of a strongly dilute polymer solution (i.e., with $D = 0.0018$).[36] Using $k = 11$ and $D = 0.0018$ together with eq 6 in eq 5, one can compare the calculated values for $\langle t_{left} \rangle$ with the simulated ones. This comparison is shown in Figure 3. Simulation and random walk description agree with each other for $b > 10$. The deviations for small b-values can be explained by the fact that the size of the polymer is then comparable to b ($R_g(N=20) \approx 6.3$) so that the point-particle approximation is no longer valid.

In summary, the random walk calculation provides a rather accurate description of the dynamical aspects of the single-chain adsorption process on an empty wall and especially yields a quantitative understanding for the dependence of the average adsorption time on z^a_{cm} and z^b_{cm}. Since the choice of these values only affects $\langle t_{left} \rangle$, but does not influence the configurational properties of the polymer close to the wall, we typically used $z^a_{cm} = 30$, satisfying roughly $z^a_{cm} > h + R_g$ (h is the height of an equilibrated brush[28]) and $b = 10$ in the subsequent simulations.

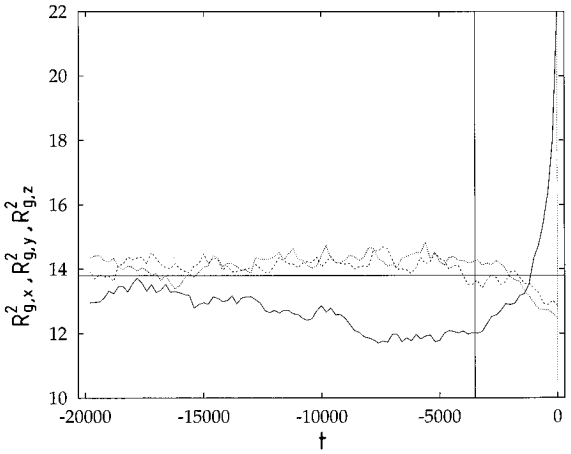

Figure 4. Components of the radius of gyration for $N = 20$ as a function of negative time: $R^2_{g,x}$ (dotted line); $R^2_{g,y}$ (dashed line); $R^2_{g,z}$ (solid line). The horizontal and vertical lines denote $R^2_g/3 \approx 13.8$ of the isolated polymer and the Rouse time $\tau_r^* \approx$ 3500 MCS.

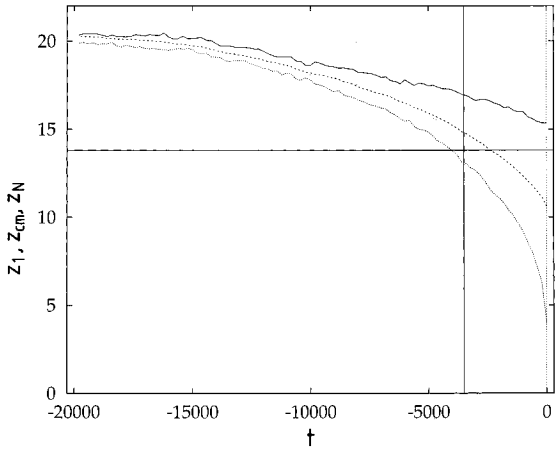

Figure 5. z-components of the center of mass z_{cm} (dashed line), of the adsorbing end monomer z_1 (dotted line), and of the other end monomer z_N (solid line) of the free polymer before adsorption at time $t = 0$ ($N = 20$). The horizontal and vertical lines denote $R^2_g/3 \approx 13.8$ of the isolated polymer and the Rouse time $\tau_r^* \approx$ 3500 MCS.

The configurational properties of the adsorbing polymer can be characterized by the components of the radius of gyration. At the moment of adsorption the components of R_g were found to be $R^2_{g,x} \approx 12$, $R^2_{g,y} \approx 12$, and $R^2_{g,z} \approx 28$ (for $N = 20$). For a strongly dilute polymer solution, Paul et al.[36] determined the radius of gyration of a free chain with $N = 20$ as $R^2_g \approx 40$, which means $R^2_{g,x} = R^2_{g,y} = R^2_{g,z} \approx 13$. This shows clearly that the polymer is highly anisotropic at the moment of adsorption. These values can also be compared with the equilibrium values of a single grafted polymer in the mushroom regime. We obtained $R^2_{g,x} \approx 13$, $R^2_{g,y} \approx 13$, and $R^2_{g,z} \approx 16$. Although the mushrooms are slightly stretched perpendicular to the surface, it is evident that the stretching of the just adsorbed chain is far more pronounced.

The development of this stretching with time is depicted in Figure 4. For times larger than about 15 000 MCS ($\approx 4\tau_r^*$) before the adsorption, the components of R^2_g coincide within the statistical uncertainties of the simulation and the average shape of the chain is spherical. This average spherical shape results from the superposition of the different spatial orientations of the chain prolate ellipsoid, which is the most probable shape of a polymer.[40] Figure 4 shows that out of all possible orientations of the ellipsoid those are favored shortly before the adsorption, which align the long axis preferentially perpendicular to the wall. In order to reach this favorable alignment for the adsorption, the ellipsoid has to turn at intermediate times ($-15\,000$ MCS $< t < -2000$ MCS) through orientations which are preferentially tilted parallel to the wall and thus exhibit a smaller R_g-component perpendicular to it. Therefore there must also be a time when the components of R_g intersect before the stretching sets in. This intersection time is about 1500 MCS before the adsorption. A glance at Figure 5, which shows the time evolution of the z-components of the upper and the lower end monomer and of the center of mass, reveals that the upper end monomer and the center of mass move only by about 1−2 lattice constants during the last 1500 MCS before adsorption, whereas the lower end monomer crosses a distance of about 10 lattice constants in the same time. In this last time interval ($t < \tau_r^*$), the motion of the (lower) end monomer is controlled by fluctuations around the average position of the monomer. Within the Rouse model, these fluctuations lead to a time dependence of $t^{1/4}$,[28] which is rather well borne out in our simulation (see section III. C.). Therefore the elongation of the adsorbed polymer along the axis perpendicular to the surface is not due to interaction with the wall but depends only on how fast and how far away from the center of mass the end monomers fluctuate before a favorable configuration leads to adsorption.

Comparing Figures 4 and 5, the following picture of the adsorption process emerges: Far away from the wall (i.e., for $t > 4\tau_r^*$), the polymer looks on average as an isotropic sphere. During the further approach toward the wall, the polymer has to reorient in such a way to bring one of the tips of its prolate ellipsoid close to the wall just before the adsorption. The adsorption takes place by a normal fluctuation of the end monomer (situated at that tip; see below) around its average position, which leads to a strong elongation of the z-component of R^2_g. This nonequilibrium stretching of adsorbed polymer relaxes on the time scale of τ_r^*, the typical relaxation time of polymers in the mushroom regime.[28]

In order for this picture to be reasonable, the end monomers have to be preferentially situated at the tips of the prolate ellipsoid. An argument in favor of this assertion stems from the observation that the first contact of the chain with the wall occurs only about 200−300 MCS before the adsorption event. Taking into account the preferential alignment of the polymer perpendicular to the wall, this means that the end monomer should have a high probability to be located at the outer edges of the polymer. In order to obtain a better insight in the position of the end monomers we first calculated the eigenvalues of the tensor of inertia $\{I_{ik}\}_{i,k=x,y,z}$, i.e., of

$$I_{ik} = \sum_{j=1}^{N} [(x_j^2 + y_j^2 + z_j^2)\delta_{ik} - i_j k_j] \qquad (8)$$

for about 1000 configurations of an isolated polymer chain and then rotated each of the polymers so that the axes with eigenvalues of comparable size are superimposed. In this way Figure 6 resulted, which shows the distribution of the end monomers along the axes of

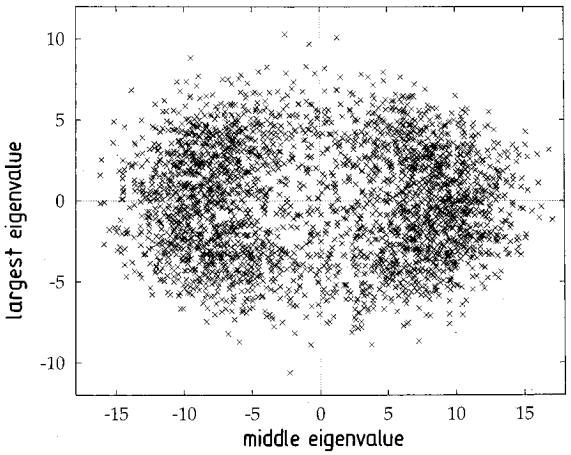

Figure 6. Projection of the distribution of the end monomers of polymers with N=20 onto the plane spanned by the eigenvectors corresponding to the largest (ordinate) and middle (abcissa) eigenvalues of the inertia tensor.

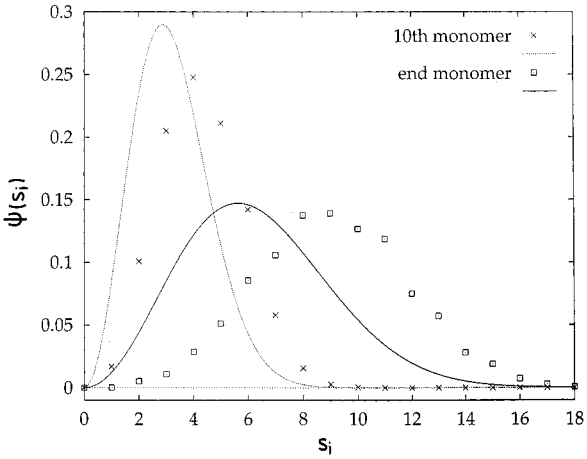

Figure 7. Comparison of the simulated radial density distribution $\psi(s_i)$ of the end and middle (10th) monomers for N = 20 with the Gaussian approximation (eq 10). s_i denotes the magnitude of the vectorial distance between the ith monomer and the center of mass. The dotted line is the Gaussian approximation for the middle monomer, the solid line for the end monomer.

the largest and the middle eigenvalues. This figure illustrates that the end monomers are more likely to be found at the tips of the polymer ellipsoid. In addition, their spatial fluctuations are larger than those of the inner monomers (the equivalent figure is not shown here). From a plot of the monomer distribution along the axes of the smallest and the middle eigenvalue (not shown), one can see that the polymer is not rotationally symmetric around the long axis, revealing the typical shape to be more like a soap than a prolate ellipsoid.

These results can be rationalized in a more quantitative fashion by calculating the radial distribution of the monomers in the frame of the center of mass for a Gaussian chain. Denoting by $\vec{s}_i$ the vectorial distance between the ith monomer and the position of the center of mass, the radial distribution is given by

$$\psi(s_i) = 4\pi s_i^2 \phi(s_i) \tag{9}$$

where

$$\phi(s_i) = \left(\frac{3}{2\pi\alpha_i b^2}\right)^{3/2} \exp\left(-\frac{3s_i^2}{2\alpha_i b^2}\right) \tag{10}$$

for a Gaussian chain. In eq 10, b^2 is the mean square bond length and α_i depends in the following way on the monomer number i

$$\alpha_i = \frac{2N^2 + 3N + 1 - 6Ni + 6i^2 - 6i}{6N} \tag{11}$$

The quantity α_i stays invariant under $i \rightarrow \mathrm{N} - i + 1$, which reflects the indistinguishability of the head and the tail of the polymer. Using $b^2 = 7.7$ for $N = 20$,[36] Figure 7 compares the Gaussian approximation with the simulation results for the radial distribution of the monomers. Although the excluded volume interaction makes the chain extend, the Gaussian approximation provides a qualitatively correct description of $\psi(s_i)$. The inner monomers have a high probability to be located inside the chain and exhibit a smaller fluctuation around their mean position, contrary to the end monomers, which are on average situated further away from the center of mass. Similar conclusions were also drawn from a renormalization group study of the segment distribution about the center of mass of an isolated polymer[29] and from detailed investigations of the asymmetry of shape of a polymer.[30−32]

B. Adsorption in a Polymer Brush. In this section the influence of a polymer brush on the adsorption behavior of a free chain is discussed. The brush was generated by randomly placing completely stretched out polymers on the wall until the desired surface coverage σ was reached and then equilibrated over about three times the time interval that the radius of gyration needs to take a stable value. During the equilibration period and the subsequent simulation, the grafting points remain fixed ("quenched disorder"). The heights h of the equilibrated brushes range between $h \approx 20.2$ for $\sigma = 0.0044$ and $h \approx 25.6$ for $\sigma = 0.071$ (for N = 20).[28] At the beginning of the simulation the center of mass of an equilibrated chain was placed at a random position in the layer $z_{\mathrm{cm}}^a = 30$, which was found to be large enough to avoid overlapping of the brush and the polymer. The cut-off border was chosen to be ten lattice sites higher (z_{cm}^b= 40) as mentioned before, and 100 different polymer configurations were used for statistical averaging.

An interesting quantity is the probability of adsorption, i.e., the splitting probability π_{left}. One expects π_{left} to decrease with increasing chemical potential of the grafted polymer chains, which scales in the semidilute regime as $\mu/k_{\mathrm{B}}T \propto (\sigma R_{\mathrm{g}}^2)^{1/2\nu}$.[28] If σ increases (at constant N), the brush becomes denser and progressively hinders the penetration of the polymer. Therefore the adsorption probability should decrease. The same applies to an increase of the chain length (at constant σ), since longer brush polymers extend over a larger region in space and thus increase the effective number of repulsive contacts with the incoming polymer (i.e., longer chains have a lower overlap density σ^*). These expectations are borne out by Figure 8, which shows the splitting probability as a function of the scaling variable σR_{g}^2, where we used $R_{\mathrm{g}}(N$=10) ≈ 4.2 and $R_{\mathrm{g}}(N$=20) ≈ 6.3. Figure 8 suggests that σR_{g}^2 might be the correct scaling variable, although the two chain lengths $N = 10$ and $N = 20$ are certainly not sufficient to prove this unambiguously. However, it is obvious that the splitting probability decreases very strongly when the number of grafted polymers increases, which

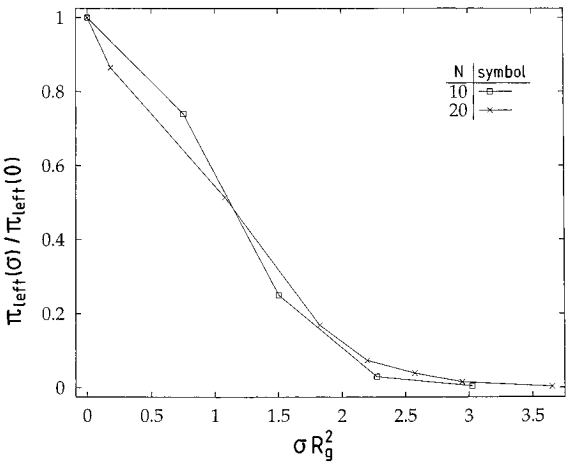

Figure 8. Plot of the scaled adsorption probability $\pi_{left}(\sigma)/\pi_{left}(0)$ versus σR_g^2 for $N = 10$ and $N = 20$. $\pi_{left}(0)$ is the adsorption (splitting) probability onto an empty surface, discussed in section II.

is the reason why it was not possible to work with grafting densities larger than $\sigma = 0.071$ in the present simulation. Certainly, this drastic decrease of π_{left} is also responsible for the long times needed to generate an equilibrated brush as observed in many experiments and simulations and as predicted by theory.[21,22,24−27]

In order to characterize the adsorption process in more detail, it is helpful to use an analogy to a similar quantum mechanical problem: The interaction of the polymer with the brush qualitatively corresponds to the interaction of a wave packet with a potential barrier. This quantum mechanical problem can be analyzed by calculating the reflection and the transmission coefficients, which measure the probability of the wave packet to be reflected by or transmitted over the potential barrier. Since the polymer cannot only penetrate the brush (transmission) or be expelled by the brush (reflection) but can also adsorb, an adsorption coefficient has to be introduced additionally. These three coefficients are defined in the following way: Let $n_{z,tot}$ be the total number of polymers whose center of mass reaches the height z above the wall, $n_{z,ref}$ the number of polymers whose center of mass penetrates the brush up to z before they are expelled, $n_{z,ad}$ the number of monomers which adsorb when their center of mass is at z, and $n_{z,trans}$ the number of monomers which neither adsorb nor leave the brush after their center of mass was at z. Then the adsorption coefficient $A(z)$, the reflection coefficient $R(z)$, and the transmission coefficient $T(z)$ may be defined as

$$A(z) = \frac{n_{z,ad}}{n_{z,tot}}, \qquad R(z) = \frac{n_{z,ref}}{n_{z,tot}}, \qquad T(z) = \frac{n_{z,trans}}{n_{z,tot}}$$
$$\text{with } A(z) + R(z) + T(z) = 1 \quad (12)$$

Figure 9 shows the quantities $A(z)$, $R(z)$, and $T(z)$ for $N = 20$ and $\sigma = 0.071$, the largest surface coverage at which sufficient statistics could be gathered ($\pi_{left}(0.071) = 0.6\%$). Adsorption starts to become important at about 15 lattice constants away from the wall. This distance is much larger than the radius of gyration of the free polymer ($R_g(N=20) \approx 6.3$), which shows that the penetrating polymer is strongly stretched perpendicular to the wall. The closer the center of mass to the wall, the more important adsorption becomes. If the center of mass is at about $z = 4$, adsorption is a

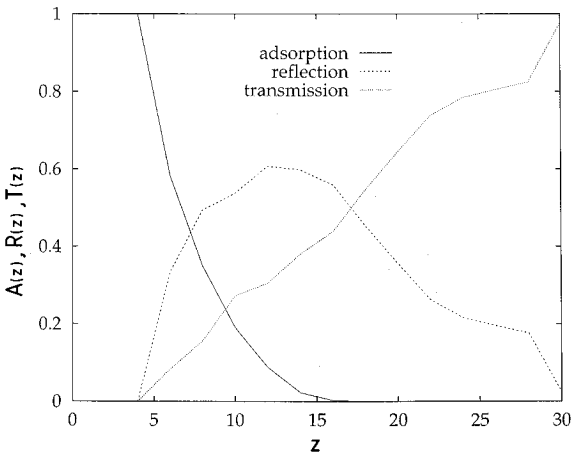

Figure 9. Plot of the adsorption $A(z)$ (solid line), reflection $R(z)$ (dashed line), and transmission $T(z)$ coefficients (dotted line) (see eq 12) versus z for $N = 20$ and $\sigma = 0.071$.

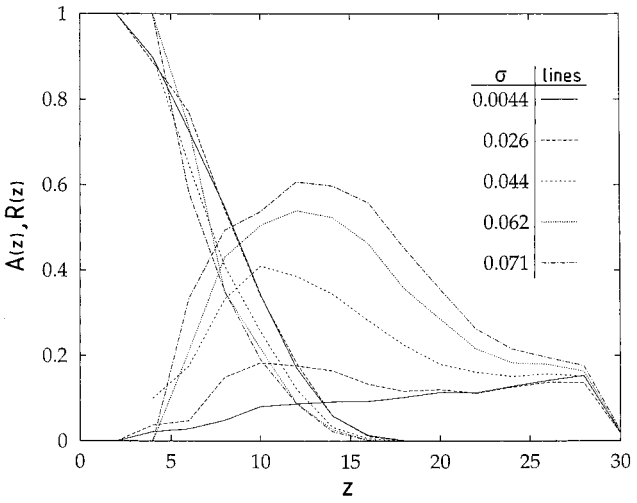

Figure 10. Adsorption $A(z)$ and reflection $R(z)$ coefficients for various surface coverages σ, i.e., $\sigma = 0.0044$ (solid line), $\sigma = 0.026$ (dashed line), $\sigma = 0.044$ (short dashes), $\sigma = 0.062$ (dotted line), and $\sigma = 0.071$ (dash-dotted line), for $N = 20$.

certain event, and both the transmission and the reflection coefficients become zero.

The reflection coefficient consists of two contributions, a stochastic contribution due to the random-walk-like motion of the penetrating polymer (contrary to the above-mentioned quantum mechanical analogue) and a contribution resulting from the interaction with the repulsive polymer brush. For a clear separation of these contributions, it is necessary to investigate the dependence of the reflectivity on different grafting densities. This is done in Figure 10, which depicts $A(z)$ and $R(z)$ for different values of σ. The adsorption coefficient varies only slightly with surface coverage, since the penetrating polymer has to approach the wall up to a certain distance to be able to adsorb, no matter what the value of σ is. Contrary to that, the reflection coefficient is strongly influenced by changes in σ. Whereas the lowest surface coverage $\sigma = 0.0044$ (i.e., one grafted polymer) virtually represents the stochastic contribution only, the repulsive interaction with the brush becomes progressively pronounced with increasing σ. For the higher surface coverages the stochastic contribution also dominates for $z \geq 29$. For these large z-values the monomer density profile is negligibly small (see Figure 11 for the profile at $\sigma = 0.071$). When the polymer further enters the brush, the reflection coef-

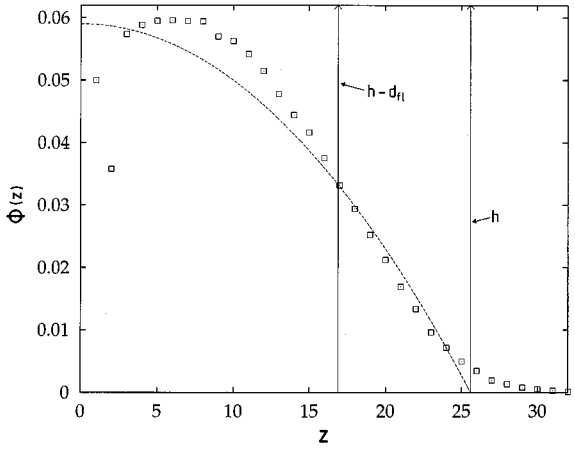

Figure 11. Monomer density profile for $\sigma = 0.071$ and $N = 20$ compared with the parabolic density $\phi(z) = \phi(0)[1 - (z/h)^2]$, where h is the brush height $h \approx 25.6$ taken from ref 28. Then normalization requires $\phi(0) = 0.059$. The two vertical lines denote $z = h$ and $z = h - d_{fl} = 16.9$.

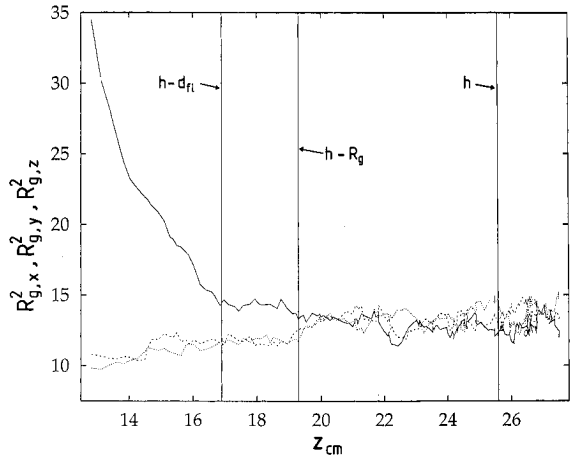

Figure 12. Plot of the x - (dotted line), y - (dashed line), and z-components (solid line) of R_g^2 for $N = 20$ and $\sigma = 0.071$ as a function of the z-position of the center of mass. The three vertical lines denote $z = h = 25.6$, $z = h - R_g = 19.3$, and $z = h - d_{fl} = 16.9$, respectively.

ficient increases and develops a maximum which shifts further away from the wall as σ becomes larger. This behavior of $R(z)$ reflects the increase of the steric repulsion with the condensation of the brush. A comparison of the reflection coefficient for $\sigma = 0.071$ in Figure 9 and the corresponding monomer profile of Figure 11 shows that the maximum of $R(z)$ has a counterpart in the monomer density profile. The maximum of the monomer density profile occurs at $z_{max} \approx 5-8$, and that of $R(z)$ at about $z \approx 12 \approx z_{max} + R_g$. For smaller z-values $R(z)$ decreases, going along with a decrease of the monomer density, and crosses $A(z)$ at $z \approx \xi(0) = (1/\sigma_g)^{1/2} = 7.5$. The z-value 7.5 corresponds to the size of the first blob.[28] In ref 28 it was found that the probability of adsorption after the desorption of a single chain becomes negligibly small if the initially anchored end monomer leaves the first blob. In analogy to that, one can expect that a fluctuation can easily lead to adsorption when the center of mass reaches the edge of the first blob and when one of the end monomers has thus to be in that blob. Therefore $A(z)$ strongly increases for $z < 7.5$.

Figure 12 depicts the components of R_g^2 for $N = 20$ and $\sigma = 0.071$ as a function of the distance of the center of mass from the wall. This distance dependence was

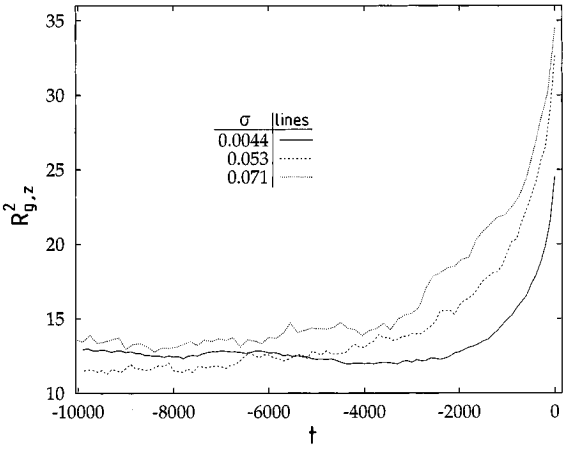

Figure 13. z-component of the radius of gyration as a function of negative time at various surface coverages, i.e., $\sigma = 0.0044$ (solid line), $\sigma = 0.053$ (dashed line), σ=0.071 (dotted line), for $N = 20$.

obtained by monitoring the time evolution of both R_g^2 and the center of mass in reverse as explained in the previous section and by eliminating the time axis by the corresponding z-position of the center of mass. Taking into account $h \approx 25.6$ and $R_g \approx 6.3$, the stretching of the penetrating polymer sets in when the center of mass is at about $z \approx 20 \approx h - R_g$ and becomes progressively pronounced when the center of mass enters the region $z \leq 17$. This finding can be rationalized in the following way: At the outer edge of the brush there is a region where the polymers are less densely packed than at the wall and where concentration fluctuations dominate. The size d_{fl} of this "dilute" region can be estimated as $d_{fl} \approx 8.7$.[28] Therefore the adsorbing polymer can initially penetrate the brush without distortion. However, when the center of mass is at $z \approx 20$, the edge of the entering polymer is at $z \approx 17 \approx h - d_{fl}$ and thus in contact with the denser portion of the brush. This induces the stretching of the polymer, which starts to increase strongly as soon as the main portion of the polymer enters this denser portion, i.e., as soon as the center of mass is at $z \approx h - d_{fl}$.

The development of this stretching as a function of time is exemplified in Figure 13 by the z-component of R_g^2 for three different surface coverages ($\sigma = 0.0044$, 0.053, 0.071). Whereas the smallest σ-value still exhibits the shallow minimum which was also found for the adsorption at an empty surface and attributed to the reorientation of the polymer ellipsoid in the previous section, the z-component of R_g^2 increases steadily for the larger surface coverages. The absence of the minimum can be explained by the fact that the center of mass of the adsorbing polymer has already deeply entered the brush (for $\sigma = 0.071$ $z_{cm} = h$ at about $t =$ 19 000 MCS; corresponding figure not shown here) so that a simple spatial reorientation without distortion of the polymer's shape is hindered by the surrounding brush chains.

C. Comparison of Adsorption and Desorption. In this section the dynamic properties of the adsorption will be compared in more detail with those of the desorption.[28] Note first that the system of the brush and the adsorbing or desorbing chain is locally in equilibrium. Therefore detailed balance applies. This implies that the probability of entering compared to the probability of leaving the brush is reduced by a factor of $\exp[-\beta\Delta\mu]$, where $\Delta\mu$ is the local difference in the chemical potential. Except for these different weights

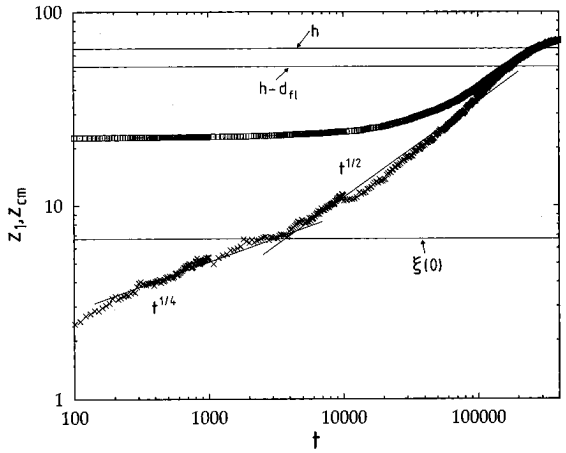

Figure 14. Double-logarithmic plot of the desorption of a polymer ($N = 50$) from a semidilute brush with surface coverage $\sigma = 0.088$. The figure shows the motion of the z-component z_1 of the cut-off end monomer (×) and the z-component z_{cm} of the center of mass (□). In addition, the expected $t^{1/4}$ and $t^{1/2}$ power laws are shown. The two power laws crossover at the edge of the first blob, i.e., at $z \approx \xi(0) = [1/\sigma_g]^{1/2} = 6.7$ (solid horizontal line). In addition, two other horizontal lines are shown for $z = h = 64.8$ and $z = h - d_{fl} = 52.4$.

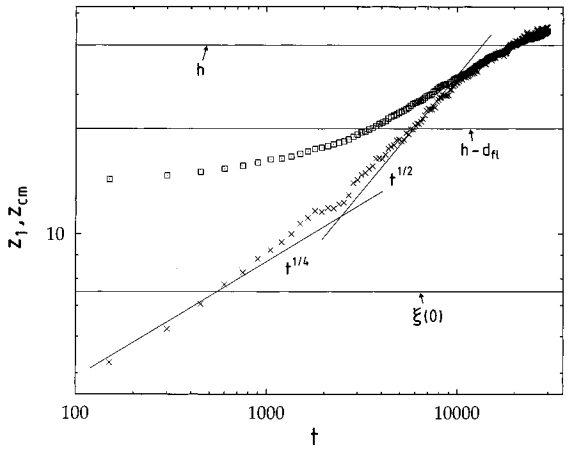

Figure 15. Double-logarithmic plot of the adsorption of a polymer ($N = 20$) in a semidilute brush with surface coverage $\sigma = 0.071$. The figure shows the motion of the adsorbing end monomer (×) and of the center of mass (□). In addition, the expected $t^{1/4}$ and $t^{1/2}$ power laws are shown. The three horizontal lines denote $z = h = 25.6$, $z = h - d_{fl} = 16.9$, and $z = \xi(0) = [1/\sigma_g]^{1/2} = 7.5$, respectively.

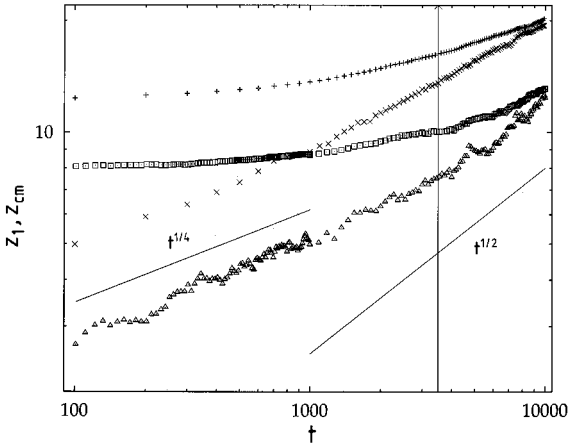

Figure 16. Comparison of the desorption and adsorption processes at $\sigma = 0.044$ of a polymer with $N = 20$ in double-logarithmic plot with the following symbols: Adsorption: center of mass (+), end-monomer (×). Desorption: center of mass (□), end-monomer (△). In the figure the $t^{1/4}$ and $t^{1/2}$ power laws are indicated as solid lines. The vertical line denotes the Rouse time $\tau_r^* \approx 3500$ MCS.

of the in and out directions we expect the physics, especially the dynamic properties, of the desorption and adsorption to be the same. Therefore we review the main results which have been obtained in the study of the desorption process.[28]

The reaction coordinate for the desorption process is the position z_1 of the initially anchored monomer which is cut off at time $t = 0$. Within the first blob (i.e., for distances $z < \xi(0) = (1/\sigma_g)^{1/2}$ and times $t < \tau_{blob}$, where τ_{blob} is the diffusion time of the monomer through the first blob) forces acting on the end monomer are small compared to the thermal energy and thus fluctuations around the average z_1-position are large. Accordingly for these short times one expects a usual anomalous diffusion with $z_1(t) \propto t^{1/4}$. For $t > \tau_{blob}$ fluctuations become unimportant and the end monomer is pulled away from the wall by the tensional force that contracts the chain. This force is independent of chain length, which is expressed by the exponent of the scaling relationship $z_1(t)/h \propto (t/\tau_{cm})^{1/2}$ for $\tau_{blob} < t < \tau_{cm}$, where $\tau_{cm} \propto \tau_d \propto N^2$ is the time that the chain's center of mass needs to reach the edge of the brush at $z = h$. Before entering the dilute part of the brush at $z = h - d_{fl}$, the chain is expelled at a constant velocity. In the dilute part of the brush, i.e., in the last blob, the chain becomes isotropic and diffuses freely.

In order to compare these results with those of the adsorption process, Figure 15 depicts the time dependence of the center of mass and of the adsorbing end monomer for $\sigma = 0.071$, the highest studied surface coverage which corresponds to a semidilute brush according to the discussion of section II. When the adsorbing polymer reaches $z \approx h - R_g$, the motion of the center of mass and of the end monomer separate and the chain becomes anisotropic (see Figure 12). For $z < h - d_{fl}$ the center of mass slows down strongly, whereas the adsorbing end monomer approaches the wall according to the expected sequence of the $t^{1/2}$ and $t^{1/4}$ behaviors. The crossover between the $t^{1/2}$ and $t^{1/4}$ behaviors occurs at $z > \xi(0)$ and thus somewhat further outside of the first blob compared to the above-described example for the desorption process. But, qualitatively, both the desorption process and the adsorption process have the same time dependence.

A possible cause for this could be a difference in the averaging procedure employed in the study of the desorption and adsorption processes. In the present simulation, every end monomer which touches the wall adsorbs, whereas in the study of the desorption the once cut-off end monomer was allowed to bounce back to the wall without readsorbing. For these monomers the wall is merely impenetrable. The contribution of these monomers to the average motion should decrease the distance that the desorbing end monomer can cover. Therefore one might expect the crossover from the $t^{1/4}$ to the $t^{1/2}$ behavior for the desorption process also to occur for $z > \xi(0)$ when from all desorbing chains a subensemble is chosen, comprising all chains which never return to the wall after being cut off.

Another question in this context is to what extent these results obtained for semidilute brushes can be transferred to the mushroom regime. Figure 16 therefore compares the desorption process with the adsorption process of a chain with $N = 20$ at $\sigma = 0.044$. In the mushroom regime the Rouse time ($\tau_r^* \approx 3500$ MCS

for $N = 20$) and the radius of gyration ($R_g \approx 6.3$ for $N = 20$) are the only relevant length and time scales. Therefore deviations from the above-described sequence of time dependences are to be expected. Nevertheless, the short-time $t^{1/4}$ behavior of the end monomer is found for $t < \tau_r^*$ for both desorption and adsorption. For longer times the $t^{1/2}$ behavior cannot be confirmed unambiguously. This is, however, to be expected, since the $t^{1/2}$ behavior is derived under the assumption of strongly stretched grafted chains, which is not satisfied in the mushroom regime. The differences in the absolute values of the individual adsorption and desorption curves may again be attributed to the reasons discussed above.

IV. Summary and Outlook

In this paper the adsorption process of a polymer in a polymer brush was studied by Monte Carlo simulation. The main results can be summarized as follows: (1) The adsorption of a free polymer onto an empty surface is analogous to the random walk of a point particle with absorbing boundaries in one dimension if the finite extension of the polymer is taken into account and if the polymer is not too close to the wall, where the point-particle approximation is no longer valid. (2) Irrespective of the surface coverage and chain length, the final step of the adsorption is governed by fluctuations of the end monomers, leading to a very anisotropic conformation at the moment of adsorption, where the polymer is strongly stretched perpendicular to the wall. This stretching is even more pronounced than that of the equilibrated brush polymers. (3) When the brush becomes denser, the steric repulsion progressively hinders the free polymer from adsorbing. This effect can clearly be seen in the splitting probability, which decreases with increasing surface coverage. The smaller the splitting probability, the more seldom adsorption takes place, which prevented simulations for $\sigma > 0.071$. The larger σ, the earlier the polymer begins to stretch and the stronger it is stretched at the moment of adsorption. (4) A comparison of the adsorption with the desorption of the single chain from the brush showed that the end monomer motion behaves as $t^{1/4}$ for short times in both processes irrespective of N and σ. The $t^{1/2}$ behavior found in the desorption process for longer times was only rather pronounced for $\sigma = 0.071$ in our study. This can be understood by the fact that the $t^{1/2}$ power law is calculated under the assumption of strongly stretched chains, i.e., of a semidilute polymer brush, a condition which is not satisfied for $\sigma < 0.071$ and $N = 20$ in our simulation.

In the future we plan to study the replacement of a long grafted layer by the introduction of shorter chains with the same head group. This effect has already been seen in experiments[23] and simulations.[26,27] Nevertheless, the microscopic replacement mechanism is not yet fully understood and a detailed simulation could probably elucidate this process further.

Acknowledgment. We are indebted to Prof. J.-F. Joanny for helpful discussions and to V. Tries for his technical assistance during the various stages of this work. J.B. and J.W. thank the Bundesministerium für Forschung und Technologie (BMFT) for financial support under Grant Nos. 03M4076 and 03M4040.

References and Notes

(1) Halperin, A.; Tirrell, M.; Lodge, T. P. *Adv. Polym. Sci.* **1992**, *31*, 100.

(2) Napper, D. H. *Polymer Stabilization of Colloidal Dispersions*; Academic Press: London, 1983.

(3) Sanchez, I. C., Ed. *Physics of Polymer Surfaces and Interfaces*; Butterworth-Heinemann: Boston, 1992.

(4) Fleer, G. J.; Cohen Stuart, M. A.; Scheutjens, J. M. H. M.; Cosgrove, T.; Vincent, B. *Polymers at Interfaces*; Chapman and Hall: London, 1993.

(5) Grest, G. S.; Murat, M. In *Monte Carlo and Molecular Dynamics Simulations in Polymer Science*; Binder, K., Ed.; Oxford University Press: New York, 1995.

(6) Taunton, H. J.; Toprakcioglu, C.; Fetters, L. J.; Klein, J. *Macromolecules* **1990**, *23*, 571.

(7) Klein, J.; Perahia, D.; Warburg, S. *Nature (London)* **1991**, *352*, 143.

(8) Alexander, S. *J. Phys. (Fr.)* **1977**, *38*, 983.

(9) de Gennes, P.-G. *J. Phys. (Fr.)* **1976**, *37*, 1434. de Gennes, P.-G. *Macromolecules* **1980**, *13*, 1069.

(10) Milner, S. T.; Witten, T. A.; Cates, M. E. *Macromolecules* **1988**, *21*, 2610.

(11) Milner, S. T.; Wang, Z.-G.; Witten, T. A. *Macromolecules* **1989**, *22*, 489.

(12) Johner, A.; Joanny, J.-F. *J. Chem. Phys.* **1993**, *98*, 1647.

(13) Witten, T. A.; Leibler, L.; Pincus, P. A. *Macromolecules* **1990**, *23*, 829.

(14) Auroy, P.; Auvray, L.; Léger, L. *Phys. Rev. Lett.* **1991**, *66*, 719.

(15) Lai, P.-Y.; Binder, K. *J. Chem. Phys.* **1991**, *95*, 9288.

(16) Lai, P.-Y.; Binder, K. *J. Chem. Phys.* **1992**, *97*, 586.

(17) Marko, J. F.; Chakrabarti, A. *Phys. Rev. E* **1993**, *48*, 2739.

(18) Wijmans, G. M.; Scheutjens, J. M. H. M.; Zhulina, E. B. *Macromolecules* **1992**, *25*, 2657.

(19) Laradji, M.; Guo, H.; Zuckermann, M. J. *Phys. Rev. E* **1994**, *49*, 3199.

(20) Lai, P.-Y.; Binder, K. *J. Chem. Phys.* **1993**, *98*, 2366.

(21) Tassin, J. F.; Siemens, R. L.; Tang, W. T.; Hadziioannou, G.; Swaler, J. D.; Smith, B. A. *J. Chem. Phys.* **1989**, *93*, 2106.

(22) Motschmann, H.; Stamm, M.; Topracioglu, C. *Macromolecules* **1991**, *24*, 3681.

(23) Kumacheva, E.; Klein, J.; Pincus, P.; Fetters, L. J. *Macromolecules* **1993**, *26*, 6477.

(24) Johner, A.; Joanny, J. F. *Macromolecules* **1990**, *23*, 5299.

(25) Milner, S. T. *Macromolecules* **1992**, *25*, 5487.

(26) Lai, P.-Y. *J. Chem. Phys.* **1993**, *98*, 669.

(27) Zajac, R.; Chakrabarti, A. *Phys. Rev. E* **1994**, *49*, 3069.

(28) Wittmer, J.; Johner, A.; Joanny, J.-F.; Binder, K. *J. Chem. Phys.* **1994**, *101*, 4379.

(29) Schäfer, L.; Krüger, B. *J. Phys. (Fr.)* **1988**, *49*, 749.

(30) Rudnick, J.; Gaspari, G. *J. Phys. A: Math. Gen.* **1986**, *19*, L191.

(31) Aronovitz, J. A.; Nelson, D. R. *J. Phys.* **1986**, *47*, 1445.

(32) Cannon, J. W.; Aronovitz, J. A.; Goldbart, P. *J. Phys. I* **1991**, *1*, 629.

(33) Deutsch, H.-P.; Binder, K. *J. Chem. Phys.* **1991**, *94*, 2294. Carmesin, I.; Kremer, K. *Macromolecules* **1988**, *21*, 2819.

(34) Binder, K.; Lai, P.-Y.; Wittmer, J. *Faraday Discuss. Chem. Soc.* **1994**, *98*, 97.

(35) Wittmer, J.; Johner, A.; Joanny, J.-F. *Colloids Surf. A: Physicochem. Eng. Aspects* **1994**, *86*, 85.

(36) Paul, W.; Binder, K.; Heermann, D.; Kremer, K. *J. Phys. II* **1991**, *1*, 37.

(37) van Kampen, N. G. *Stochastic Processes in Physics and Chemistry*; North-Holland: Amsterdam, 1987.

(38) Feller, W. *An Introduction to Probability Theory and its Applications*; Wiley: New York, 1968.

(39) Weiss, G. H. *Aspects and Applications of the Random Walk*; North-Holland: Amsterdam, 1994.

(40) Doi, M.; Edwards, S. F. *The Theory of Polymer Dynamics*; Clarendon Press: Oxford, 1986.

MA951083K